

## Formation of Nanotwins in Proton-Irradiated Austenitic 316 Stainless Steel

Yun Soo Lim\*, Dong Jin Kim, Sung Sik Hwang, Sung Woo Kim, Min Jae Choi, Sung Hwan Cho  
Materials Safety Technology Research Division, Korea Atomic Energy Research Institute  
1045 Daedeok-daero, Yuseong-gu, Daejeon 305-353, Korea  
\*Corresponding author: yslim@kaeri.re.kr

### 1. Introduction

Austenitic 316 stainless steel (SS) is a common structural material used in pressurized water reactor (PWR) components. The radiation environment in a reactor causes substantial degradation in the properties of SS and can lead to premature failures. The failure mechanism of a core component manufactured by austenitic 316 SS in the PWR environment is still not well understood due to its intrinsic complexity; however, it appears that microstructural and microchemical alterations by neutron irradiation are the key variables responsible for the component failure. Therefore, studies of radiation-induced microstructural and microchemical changes should be the first step to understand how irradiation defects affect the failures of this alloy.

Proton irradiation has attracted much attention in the study of radiation-induced degradation phenomena instead of neutron irradiation. Proton irradiation is a useful experimental technique for simulating neutron radiation-induced phenomena in nuclear core materials despite some limitations [1]. Under the proper irradiation conditions, proton irradiation can produce a microstructure and microchemistry very similar to those by neutron irradiation [2]. Proton irradiation creates a variety of irradiation defects such as vacancies/interstitials, Frank loops, network dislocations, voids and so on, from which radiation-induced microstructural changes occur as well [3]. However, formation of nanotwins in austenitic 316 SS by proton irradiation has not been reported yet in the literature.

In the present study, nanotwins found using transmission electron microscopy (TEM) in proton-irradiated austenitic 316 SS is presented. Nanotwins found in the proton-irradiated 316 SS are confirmed by several methods to make sure that they were induced by proton irradiation itself, not by sample preparation process for microscopic study. Finally, possible formation mechanism for nanotwins in austenitic 316 SS by proton irradiation is briefly discussed

### 2. Methods and Results

#### 2.1 Material and Proton Irradiation

Table 1. Composition of the austenitic 316 SS (wt%)

Cr	Ni	C	Mo	Mn	Si	Cu	P	Fe
16.1	10.4	0.047	2.11	1.08	0.66	0.1	0.003	Bal.

Austenitic 316 SS was used in this study, and the chemical composition of the alloy is given in Tables 1. The test alloy was solution annealed at 1100 °C and finally water quenched. Before proton irradiation, the surfaces of the specimens were mechanically ground and then electrochemically polished in a solution of 50 vol% phosphoric acid + 25 vol% sulfuric acid + 25 vol% glycerol for 15 - 30 s at room temperature. The proton irradiation was performed with the General Ionex Tandatron accelerator at the Michigan Ion Beam Laboratory at the University of Michigan. The irradiation processes were conducted using 2 MeV protons at a current range of 40  $\mu$ A. The specimens were exposed at 360 °C to four levels of irradiation of 0.4, 1.6, 2.7, and 4.2 displacements per atom (dpa) at a depth of 10  $\mu$ m from the surface, which will be referred as A, B, C and D specimens hereafter. The radiation damage levels of the samples were calculated with the Stopping and Range of Ions in Matter (SRIM) program using a displacement energy of 40 eV in the 'quick calculation' mode.

#### 2.2 Sample Preparation and Microstructural Analysis

The specimens for optical microscopy and SEM were prepared by chemical etching in a solution of 2 vol% bromine+98 vol% methanol. TEM foils containing the irradiated area were prepared with conventional electro-polishing (EP) method. To prepare the TEM specimens, thin foils were mechanically thinned until they were less than 40  $\mu$ m thick and then electro-jet polished in a 7 vol% perchloric acid + 93 vol% methanol solution at -40 °C with a current of approximately 80 mA. The focused ion beam (FIB) TEM specimens of the proton-irradiated austenitic 316 SS were also prepared using a dual-beam Hitachi FIB-2100 system with Ga ions with an incident beam energy level of 30 kV and a current of 1 - 5 nA. Final thinning was done at an acceleration voltage of 5 kV to eliminate the surface damage produced by highly energetic ions during the FIB milling process.

The proton-irradiated specimens were investigated using various types of microscopic equipment. The SEM imaging and orientation imaging microscopy (OIM) by electron back-scattered diffraction (EBSD) were done with a JEOL 6300 (operating voltage 20 kV). TEM analysis was done with a JEOL JEM-2100F

(operating voltage 200 kV) to determine the irradiation-defects including nanotwins due to proton irradiation.

### 2.3 TEM Results on the nanotwins

The irradiation damages depending on the dpa and the depth of 316 SS were calculated with the Stopping and Range of Ions in Matter (SRIM) 2008 program using a displacement energy of 40 eV in the 'quick calculation' mode. These results are given in Fig. 1. The damage profiles exhibit a slow increase roughly up to a depth of 15  $\mu\text{m}$ , as well as subsequent damage peaks near the depth of 20  $\mu\text{m}$  from the irradiated surfaces.

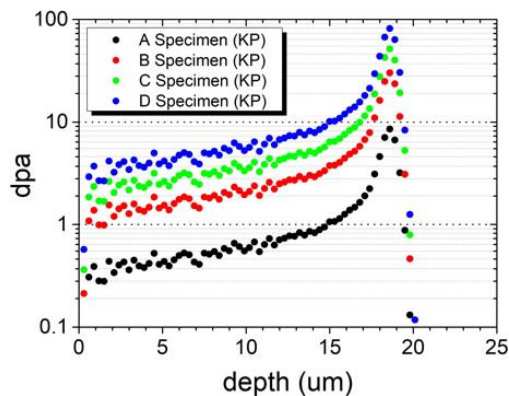


Fig. 1. Calculated dpa-depth profiles of the proton-irradiated 316 SS using the 'quick calculation' mode of SRIM program.

Fig. 2 presents the microstructural features of the austenitic 316 SS under test before proton irradiation. Parallel fringes, a signature of stacking faults, are readily observable in the TEM bright field (BF) image, as shown in Fig. 2. Austenitic 316 SS has a low stacking fault energy (SFE) [4]; therefore, twins as well as stacking faults can easily be generated. The dislocation density was very low, where the image was obtained in a two-beam condition with a  $B \sim [110]$  zone axis.



Fig. 2. TEM BF image of stacking faults and dislocations in the austenitic 316 SS before proton irradiation.

Fig. 3 shows a TEM BF image of nanotwins produced in a proton-irradiated specimen that

underwent a dose of 4 dpa in B specimen. This TEM specimen was obtained by EP treatment method. The twins found in this specimen had a nano-sized thickness. The orientation relationship between the austenitic 316 SS and the nanotwins was clearly demonstrated in the inserted diffraction pattern in the figure when the electron beam was in the [011] direction. Nanotwins were also found in the specimens underwent a dose of 1 dpa in EP-treated A, and 6 dpa in EP-treated D specimens.

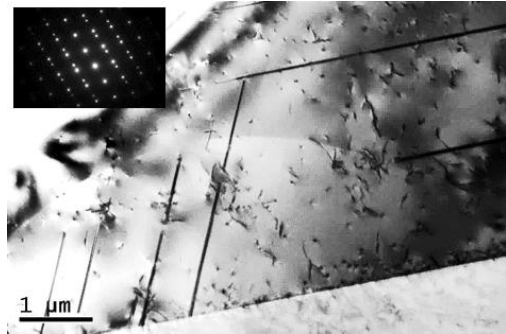


Fig. 3. TEM BF image showing nanotwins in austenitic 316 SS proton-irradiated with a dose of 1.6 dpa.

These types of nanotwins in proton-irradiated austenitic 316 SS have not been reported yet in the literature. They were not found in the specimens before proton irradiation in the present study either. Only some fringes originating from stacking faults in the TEM images were visible, as shown in Fig. 2. Therefore, it appears that the nanotwins were formed by the proton irradiation itself and/or by mechanical damage introduced during the TEM sampling preparation process after proton irradiation. FIB lift-out TEM specimens were taken directly from the as-irradiated surface such that any types of possible mechanical damage could be completely excluded during the sampling preparation process. In this way, it could be more clearly verified whether or not mechanical damage was induced during the preparation process of the EP-treated TEM specimens.

Fig. 4 presents the results obtained from an FIB lift-out TEM sample directly taken from the as-irradiated surface of specimen A. Fig. 4(a) is a TEM BF image with an electron beam direction on the [110] zone axis. A diffraction pattern obtained from the region denoted by a yellow circle in Fig. 4(a) was presented, and it revealed clearly that the dark line set in the figure had a twin relationship with the matrix. Fig. 4(b) is a dark field (DF) image of the nanotwins taken from the twin spot in the diffraction pattern of Fig. 4(a). In many cases, a thick nanotwin was composed of a bundle of nanotwins, with each nanotwin in the bundle having a different thickness, as shown in Fig. 4(b). From all of these results, it can be confirmed that the nanotwins

found in the proton-irradiated specimens (Figs. 3 and 4) were generated by the proton-irradiation itself.

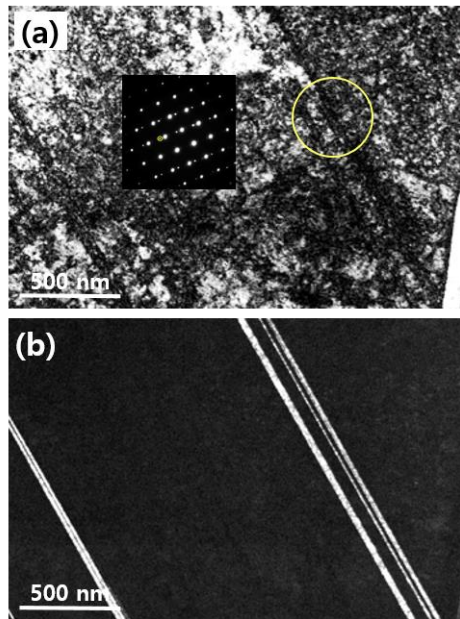


Fig. 4. (a) TEM BF image and diffraction pattern, and (b) DF image of nanotwins found in the FIB lift-out TEM specimen taken directly from the as-irradiated surface of specimen A.

#### 2.4 Possible Formation Mechanism for Nanotwins in Proton-Irradiated Austenitic 316 SS

Based on the results obtained in this study, a possible twinning process in austenitic 316 SS under irradiation will be discussed. Twinning in irradiated 316 SS can occur by a moving perfect dislocation dissociates into Shockley partial dislocations with a  $\langle 112 \rangle / 6$  Burgers vectors gliding on successive  $\{111\}$  slip planes, which is a basic theory to explain the deformation twinning of fcc metals and alloys. Irradiation induces stress inside the material, referred to as radiation-induced stress [5] or internal stress [6]. This stress can be operative for the entire period of irradiation by producing point defects continuously. The shear component of the irradiation-induced or internal stress appears to serve as the driving force to move dislocations for the nucleation and growth of nanotwins in irradiated austenitic 316 SS even with no external load or stress.

The nucleation of nanotwins in proton-irradiated 316 SS appears to be caused by the easy formation of stacking faults owing to the low SFE of this alloy [4]. Stacking faults that exist before proton irradiation (Fig. 2) can promote the nucleation process of nanotwins more effectively. As proton irradiation proceeds, previously formed twins grow while new twins are nucleated, increasing the number density of the nanotwins and making the individual nanotwins thicker. The closely separated nanotwins nucleate sequentially and grow independently, and they compose a bundle of

nanotwins with different thicknesses (Fig. 4(b)). Nanotwins formed by proton irradiation in 316 SS has not yet been reported in the literature; therefore, there is a lack of information about the twinning mechanism in this alloy under irradiation. More rigid and through studies to reveal the twinning mechanism in austenitic 316 SS under irradiation are necessary.

### 3. Conclusions

In the present work, austenitic 316 SS specimens were irradiated using 2 MeV protons with an average dose rate of  $\sim 7.1 \times 10^{-6}$  dpa/s at 360 °C and nanotwins induced by proton irradiation were characterized using EP-treated and FIB TEM specimens. The following conclusions were derived from the present study.

1. The test alloy before proton irradiation had a homogeneous and isotropic microstructure with many annealing macrotwins. Stacking faults were frequently found owing to the low SFE of this alloy.

2. Twins were found in EP-treated B specimen underwent a dose of 4 dpa, and they had a nano-sized thickness. From the analysis of diffraction patterns, it was clearly identified that the nanotwins and the matrix had a typical twin relationship. Nanotwins were also found in the specimens underwent a dose of 1 dpa in EP-treated A, and 6 dpa in EP-treated D specimens.

3. Nanotwins were also identified in the FIB lift-out TEM specimens, which were taken directly from the as-irradiated surface such that any types of possible mechanical damage could be completely excluded during the sampling preparation process. Therefore, it can be concluded that nanotwins found in the proton-irradiated austenitic 316 SS specimens were generated by the proton-irradiation itself.

### REFERENCES

- [1] S.J. Zinkle, and L.L. Snead, Opportunities and limitations for ion beams in radiation effects studies: bridging critical gaps between charged particle and neutron irradiations, *Scr. Mater.* Vol. 143, p. 154, 2018.
- [2] J. Gan, and G. Was, Microstructure evolution in austenitic Fe-Cr-Ni alloys irradiated with protons: comparison with neutron-irradiated microstructures, *J. Nucl. Mater.* Vol. 297, p. 161, 2001.
- [3] S.J. Zinkle, Radiation-induced effects on microstructure, *Comprehensive Nuclear Materials Vol. 1*, Elsevier, pp. 65–98, 2012.
- [4] R.E. Schramm, and R.P. Reed, Stacking fault energies of seven commercial austenitic stainless steels, 316 SS stacking fault energy, *Metall. Trans. A.* Vol. 6A, p. 1345, 1975.
- [5] M. Sniureviciue, J. Laurikaitiene, D. Adliene, L. Augulis, Z. Rutkuniene, and A. Jotautis, Stress and strain in DLC films induced by electron bombardment, *Vacuum* Vol. 83 p. S159, 2009.
- [6] R. Ning, Z.P. Yang, Z.Y. Gao, X.Z. Cao, and W. Cai, Proton irradiation induced phase transformation in Ni-Mn-Ga thin films, *Mater. Sci. Eng.* Vol. 266, 115078, 2021.